Available online at www.sciencedirect.com
SCIENCE DIRECT®
Physics Letters B 576 (2003) 265–272
PHYSICS LETTERS B
www.elsevier.com/locate/physletb

Towards a model-independent low momentum nucleon–nucleon interaction

S.K. Bogner [a], T.T.S. Kuo [a], A. Schwenk [a], D.R. Entem [b], R. Machleidt [b]

[a] *Department of Physics and Astronomy, State University of New York, Stony Brook, NY 11794-3800, USA*
[b] *Department of Physics, University of Idaho, Moscow, ID 83844-0903, USA*

Received 1 May 2003; received in revised form 7 August 2003; accepted 4 October 2003

Editor: J.-P. Blaizot

Abstract

We provide evidence for a high precision model-independent low momentum nucleon–nucleon interaction. Performing a momentum-space renormalization group decimation, we find that the effective interactions constructed from various high precision nucleon–nucleon interaction models, such as the Paris, Bonn, Nijmegen, Argonne, CD Bonn and Idaho potentials, are identical. This model-independent low momentum interaction, called $V_{\mathrm{low\,k}}$, reproduces the same phase shifts and deuteron pole as the input potential models, without ambiguous assumptions on the high momentum components, which are not constrained by low energy data and lead to model-dependent results in many-body applications. $V_{\mathrm{low\,k}}$ is energy-independent and does not necessitate the calculation of the Brueckner G matrix.

PACS: 21.30.Cb; 21.60.-n; 21.30.Fe; 11.10.Hi

Keywords: Nucleon–nucleon interaction; Effective interactions; Renormalization group

1. Introduction

In low energy nuclear systems such as finite nuclei and nuclear matter, one can base complicated many-body calculations on a simple picture of point-like nucleons interacting by means of a two-body potential and three-body forces when needed. Unlike for electronic systems where the low energy Coulomb force is unambiguously determined from quantum electrodynamics, there is much ambiguity in nuclear physics owing to the non-perturbative nature of quantum chromodynamics (QCD) at low energy scales. Consequently, there are a number of high precision, phenomenological meson exchange models of the two-nucleon force V_{NN}, such as the Paris [1], Bonn [2], Nijmegen [3], Argonne [4] and CD Bonn [5,6] potentials, as well as model-independent but less accurate treatments based on chiral effective field theory (EFT) [7–10], for a review see [11]. We also study the Idaho potential [12], which is based on the EFT framework, but some model dependence is introduced in order to achieve similarly high precision as compared to the other interaction models.

E-mail addresses: bogner@phys.washington.edu (S.K. Bogner), kuo@nuclear.physics.sunysb.edu (T.T.S. Kuo), aschwenk@mps.ohio-state.edu (A. Schwenk).

0370-2693/$ – see front matter
doi:10.1016/j.physletb.2003.10.012

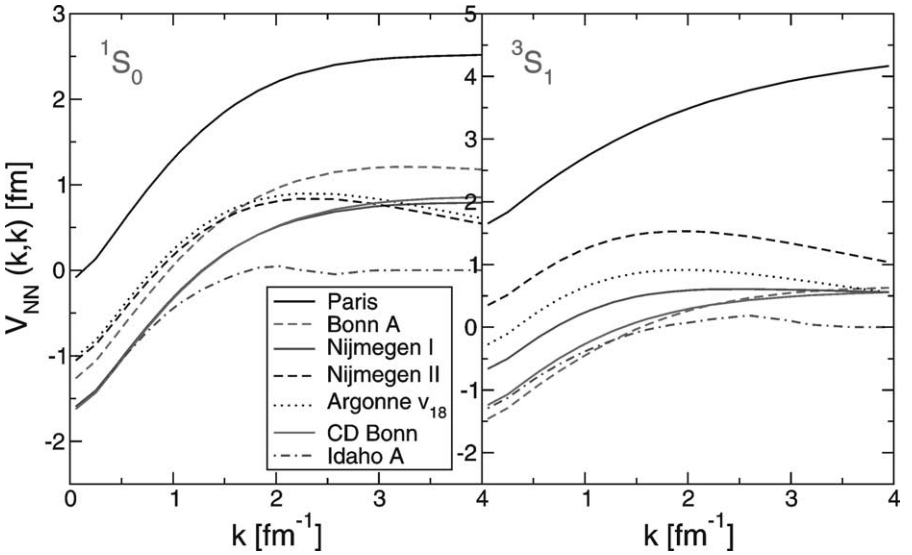

Fig. 1. Momentum-space matrix elements of $V_{\rm NN}$ for different bare potentials in the $^1S_0$ and $^3S_1$ channels.

These nuclear force models incorporate the same one-pion exchange interaction (OPE) at long distance, but differ in their treatment of the intermediate and short-range parts (e.g., parameterization of the repulsive core compared to ω exchange, different form factors, dispersive or field theoretical treatment of the 2π exchange). The fact that the different short distance constructions reproduce the same phase shifts and deuteron properties indicates that low energy observables are insensitive to the details of the short distance dynamics. The EFT approach exploits this insensitivity by explicitly keeping only the pion and nucleon degrees of freedom (in accordance with the spontaneous breaking of chiral symmetry in the QCD vacuum) and encoding the effects of the integrated heavy degrees of freedom in the form of couplings which multiply model-independent delta functions and their derivatives, see, e.g., [13]. The EFT thus provides a model-independent description of the two-nucleon system. However, the high precision, i.e., $\chi^2/\text{datum} \approx 1$, description of the nucleon–nucleon scattering data provided by conventional models is at present not achieved by the rigorous EFT potentials.

In Fig. 1, we observe that the realistic models of $V_{\rm NN}$ have quite different momentum-space matrix elements despite their common OPE parts and reproduction of the same low energy data. It demonstrates that the low energy phase shifts and deuteron properties cannot distinguish between the models used for the short distance parts. However, in many-body calculations the assumed short-distance structure of a particular $V_{\rm NN}$ enters by means of virtual nucleon states extending to high momentum, which will lead to model-dependent results, e.g., in Brueckner Hartree–Fock calculations of the binding energy of nuclear matter. It is clearly of great interest to remove such model dependence from microscopic nuclear many-body calculations.

Motivated by these observations, we perform a renormalization group (RG) decimation and integrate out the ambiguous high momentum components of the realistic interactions. Due to the separation of scales in the nuclear problem, it is reasonable to expect that the model dependence of the input potentials will be largely removed as the high momentum components are excluded from the Hilbert space. Starting from any of the $V_{\rm NN}$ in Fig. 1, we integrate out the momenta above a cutoff Λ to obtain an effective low momentum potential, called $V_{\rm low\,k}$. The physical condition is that the effective theory reproduces the deuteron pole and the half-on-shell (HOS) T matrices of the input $V_{\rm NN}$ model (i.e., the observable scattering phase shifts and the low momentum components of the two-body wave functions, which probe the OPE part of the interaction), but with all loop momenta cutoff at Λ. We will find the striking result of Fig. 2 that the $V_{\rm low\,k}$

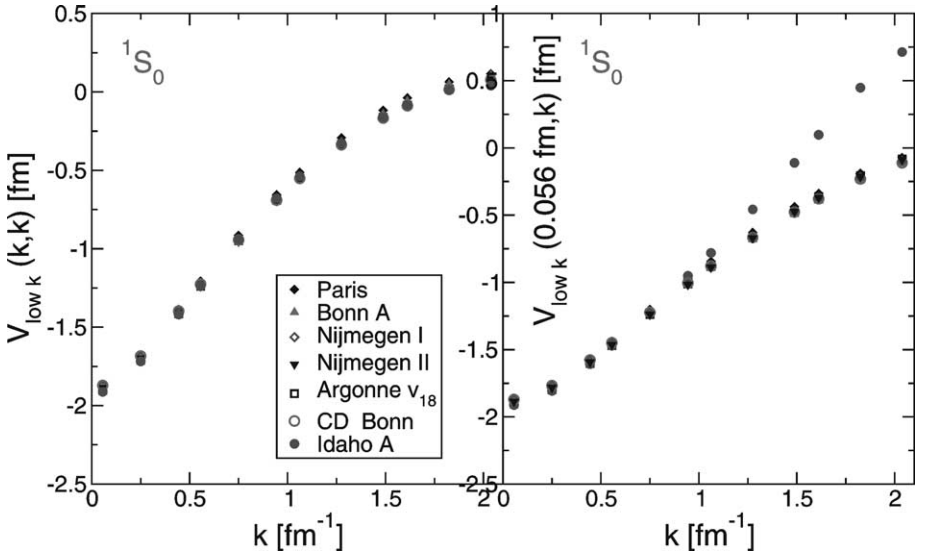

Fig. 2. Diagonal and off-diagonal momentum-space matrix elements of the $V_{\mathrm{low\,k}}$ obtained from the different bare potentials in the $^1S_0$ channel for a cutoff $\Lambda = 2.1$ fm^{-1}.

becomes independent of the particular input model for $\Lambda \lesssim 2.1$ fm^{-1}, which corresponds to laboratory energies $E_{\mathrm{lab}} \lesssim 350$ MeV. The latter is the energy scale over which the high precision potentials are constrained by experimental data.

Our strategy thus is a compromise between conventional models and EFT treatments. The resulting $V_{\mathrm{low\,k}}$ reproduces the nucleon–nucleon scattering phase shifts with similar accuracy as the high precision potentials, but without making further assumptions on the detailed high momentum structure, which cannot be resolved by fitting to the low energy data only.

2. Renormalization group decimation

The first step in the RG decimation is to define an energy-dependent effective potential (called the $\hat{Q}$ box or the Bloch–Horowitz potential in effective interaction theory), which is irreducible with respect to cutting intermediate low momentum propagators. The $\hat{Q}$ box resums the effects of the high momentum modes,

$$\hat{Q}(k',k;\omega) = V_{\mathrm{NN}}(k',k) + \frac{2}{\pi}\mathcal{P}\int_{\Lambda}^{\infty} \frac{V_{\mathrm{NN}}(k',p)\hat{Q}(p,k;\omega)}{\omega - p^2}p^2\,dp, \tag{1}$$

where k', k, and p denote the relative momentum of the outgoing, incoming, and intermediate nucleons. The principal value HOS T matrix for a given partial wave is obtained by solving the Lippmann–Schwinger equation

$$T(k',k;k^2) = V_{\mathrm{NN}}(k',k) + \frac{2}{\pi}\mathcal{P}\int_{0}^{\infty} \frac{V_{\mathrm{NN}}(k',p)T(p,k;k^2)}{k^2 - p^2}p^2\,dp. \tag{2}$$

In terms of the effective cutoff-dependent $\hat{Q}$ potential, the scattering equation can be expressed as

$$T(k',k;k^2) = \hat{Q}(k',k;k^2) + \frac{2}{\pi}\mathcal{P}\int_{0}^{\Lambda} \frac{\hat{Q}(k',p;k^2)T(p,k;k^2)}{k^2 - p^2}p^2\,dp. \tag{3}$$

The low momentum effective theory defined by Eqs. (1) and (3) preserves the low energy scattering amplitudes and bound states independently of the chosen model space, i.e., the value of the cutoff Λ. However, the energy dependence of the effective $\hat{Q}$ potential is inconvenient for practical calculations. In order to

eliminate the energy dependence, we introduce the so-called Kuo–Lee–Ratcliff folded diagrams, which provide a way of reorganizing the Lippmann–Schwinger equation, Eq. (3), such that the energy dependence of the $\hat{Q}(k', k; \omega)$ box is converted to a purely momentum dependent interaction, $V_{\mathrm{low\,k}}(k', k)$ [14,15]. The folded diagrams are correction terms one must add to Eq. (3), if one were to set all $\hat{Q}$ box energies right side on-shell. This explicitly leads to (for details see [15,16])

$$\begin{aligned} &V_{\mathrm{low\,k}}(k', k) \\ &\quad = \hat{Q}\big(k', k; k^2\big) \\ &\qquad + \frac{2}{\pi}\mathcal{P}\int_0^{\Lambda} p^2\,dp\,\hat{Q}\big(p, k; k^2\big) \\ &\qquad \times \frac{\hat{Q}(k', p; k^2) - \hat{Q}(k', p; p^2)}{k^2 - p^2} + \mathcal{O}\big(\hat{Q}^3\big). \end{aligned} \tag{4}$$

The folded diagram resummation indicated in Eq. (4) can be carried out to all orders using the similarity transformation method of Lee and Suzuki [17,18]. By construction, the resulting energy-independent $V_{\mathrm{low\,k}}$ preserves the low momentum HOS T matrix of the input V_{NN} model [19],

$$\begin{aligned} &T\big(k', k; k^2\big) \\ &\quad = V_{\mathrm{low\,k}}(k', k) \\ &\qquad + \frac{2}{\pi}\mathcal{P}\int_0^{\Lambda} \frac{V_{\mathrm{low\,k}}(k', p)T(p, k; k^2)}{k^2 - p^2} p^2\,dp, \end{aligned} \tag{5}$$

where all momenta are constrained to lie below the cutoff Λ. As our RG decimation preserves the half-on-shell T matrix, we have $dT(k', k; k^2)/d\Lambda = 0$, which implies a RG equation for $V_{\mathrm{low\,k}}$ [16]

$$\frac{d}{d\Lambda} V_{\mathrm{low\,k}}(k', k) = \frac{2}{\pi}\frac{V_{\mathrm{low\,k}}(k', \Lambda)T(\Lambda, k; \Lambda^2)}{1 - (k/\Lambda)^2}. \tag{6}$$

Similarly, a scaling equation is obtained for the $\hat{Q}$ box by integrating out an infinitesimal momentum shell, and one finds

$$\frac{d}{d\Lambda}\hat{Q}\big(k', k; p^2\big) = \frac{2}{\pi}\frac{\hat{Q}(k', \Lambda; p^2)\hat{Q}(\Lambda, k; p^2)}{1 - (p/\Lambda)^2}. \tag{7}$$

This equation was obtained previously by Birse et al. by requiring the invariance of the full-off-shell T matrix, $dT(k', k; p^2)/d\Lambda = 0$ [20].

The RG equation, Eq. (6), lies at the heart of the approach presented here: given a microscopic input model with a large cutoff, one can use the RG equation to evolve the bare interaction to a physically equivalent, but simpler effective theory valid for energies below the cutoff. The RG evolution separates the details of the assumed short distance dynamics, while incorporating their detail-independent effects on low energy phenomena through the running of the effective interaction [16,21].

The principal difference between the presented RG approach and the standard EFT one is that we do not expand the interaction in powers of local operators. This implies that, first, one does not make assumptions on locality, and that second, we do not truncate after a certain power included in the low momentum interaction. In the EFT approach, power-counting is used to calculate observables to a given order with controllable errors. In contrast, we start from a Hamiltonian in a large space, which reproduces the low energy observables with high accuracy and then decimate to a smaller, low momentum space so that the observables are reproduced. Since the exact RG equation is solved without truncation, the invariance of the T matrices is guaranteed.

Nevertheless, there are close similarities between the presented RG approach and the standard EFT one. For example, at cutoffs above the pion mass, $V_{\mathrm{low\,k}}$ keeps the pion exchange explicit, while the unresolved short distance physics could be encoded in a series of contact terms. Moreover, we find below that $V_{\mathrm{low\,k}}$ seems only to depend on the fact that all potential models have the same pion tail, and fit the same phase shifts. This is similar to EFT treatments, where the interaction is constrained by pion exchange, phase shifts and the choice of regulator.

3. Results

Referring to Fig. 2, we find the central result of this Letter. The diagonal matrix elements of $V_{\mathrm{low\,k}}$ obtained from the different V_{NN} of Fig. 1 collapse onto the same curve for $\Lambda \lesssim 2.1\ \mathrm{fm}^{-1}$. Similar results are found in all partial waves and will be reported elsewhere in detail [23]. We emphasize that $V_{\mathrm{low\,k}}$ reproduces the experimental phase shift data and the deuteron pole with similar accuracy as compared with

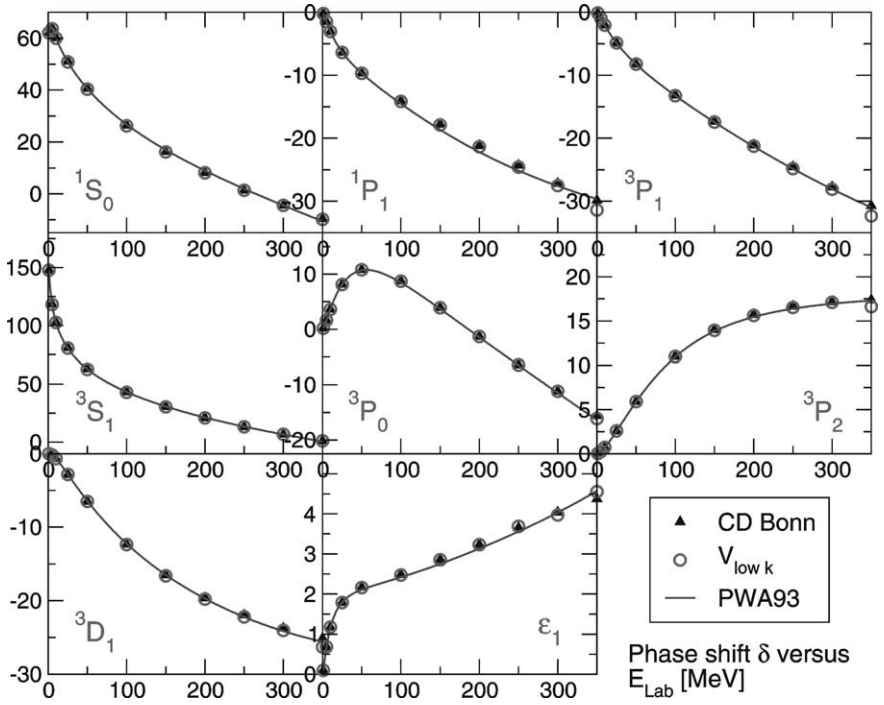

Fig. 3. S-wave (singlet and triplet with mixing parameter) and P-wave phase shifts of $V_{\mathrm{low\,k}}$ for a cutoff $\Lambda = 2.1$ fm^{-1} compared to the input V_{NN} model used, here the CD Bonn potential. We also show the results of the multi-energy phase shift analysis (PWA93) of the Nijmegen group [22]. For $V_{\mathrm{low\,k}}$ the agreement of the calculated phase shifts with the PWA93 is determined by the quality of the fit for the bare interaction.

the high precision potential models, as we show in Fig. 3. The reproduction of the phase shifts with the renormalized $V_{\mathrm{low\,k}}$ does however not require ambiguous high momentum components, which are not constrained by the low energy scattering data. We note that the change in sign of the $^1S_0$ and the $^3P_0$ phase shifts indicates that the effects of the repulsive core are properly encoded in $V_{\mathrm{low\,k}}$.

Intriguingly, the $V_{\mathrm{low\,k}}$ mainly differs from the bare potential by a constant shift. This was previously observed by Epelbaum et al. for a toy two-Yukawa bare potential [24]. The constant shift in momentum space corresponds to a smeared delta function in coordinate space and accounts for the renormalization of the repulsive core from the bare interactions, see also [25].

In Fig. 2, we find a similar behaviour for the off-diagonal matrix elements, although the $V_{\mathrm{low\,k}}$ derived from the Idaho potential begins to differ from the others at approximately $2m_\pi = 1.4$ fm^{-1}. This discrepancy in the off-diagonal matrix elements arises from the fact that the Idaho potential used here treats the 2π exchange differently than the meson models do. We can integrate out further and lower the cutoff to $\Lambda \lesssim 1.4$ fm^{-1}, then the off-diagonal elements collapse as well.

These results can be understood from T matrix preservation. The HOS T matrix determines the phase shifts as well as the low momentum components of the low energy scattering and bound state wave functions. Using the spectral representation of the T matrix, $V_{\mathrm{low\,k}}$ can be expressed as

$$V_{\mathrm{low\,k}}(k',k) = T\left(k',k;k^2\right) + \frac{2}{\pi}\mathcal{P}\int_0^\Lambda T\left(k',p;p^2\right) \times \frac{1}{p^2-k^2} T\left(p,k;p^2\right). \tag{8}$$

The V_{NN} models give the same on-shell T matrices over the phase shift equivalent kinematic range of $k \lesssim 2.1$ fm^{-1}, but their off-shell behavior is a priori unconstrained. In practice, however, one observes that

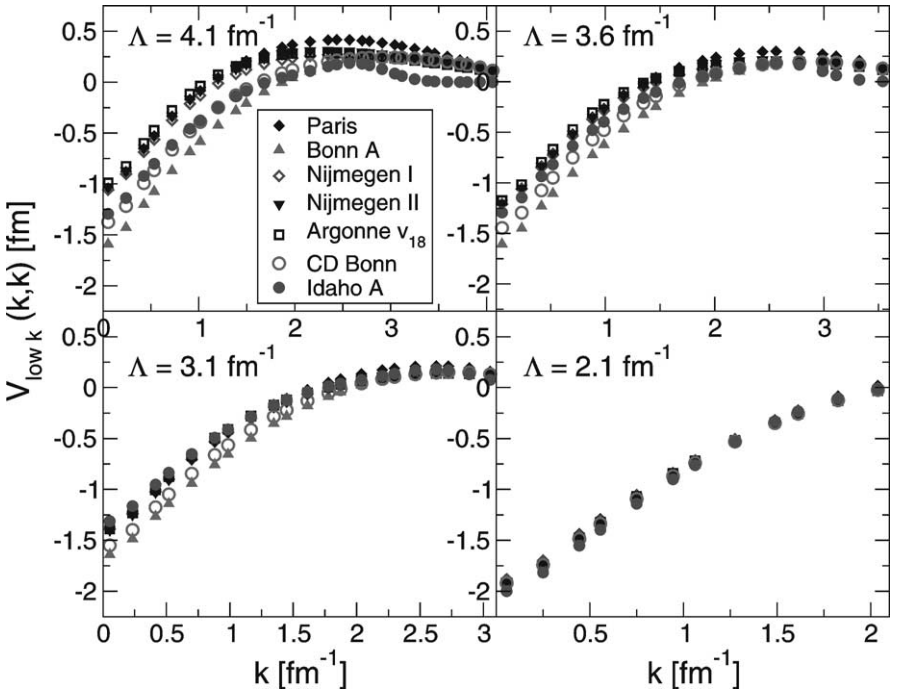

Fig. 4. Evolution of the diagonal momentum-space matrix elements for the $V_{\mathrm{low\,k}}$ derived from the different bare potentials from larger values of the cutoff to $\Lambda = 2.1$ fm^{-1} in the ^{3}S$_1$ partial wave.

the realistic potential models result in similar HOS T matrices at low energies and momenta. This is understood from the fact that these models share the same long-range OPE interaction and differ most noticeably on short-distance scales set by the repulsive core, $r \sim 0.5$ fm and smaller. Consequently, one expects that the off-shell differences are suppressed at energies and momenta below a corresponding scale of $\Lambda \sim 1/r \sim 2.0$ fm^{-1}. It is clear from Eq. (8) that the approximate HOS T matrix equivalence is a sufficient condition for the $V_{\mathrm{low\,k}}$ to be independent of the various potential models. Moreover, the spectral representation clarifies that the off-diagonal matrix elements of $V_{\mathrm{low\,k}}$ are more sensitive to a particular off-shell behavior as observed in Fig. 2, and thus deviate at a lower cutoff than the diagonal matrix elements. The collapse of the diagonal momentum-space matrix elements at the scale set by the constraining scattering data, $\Lambda \approx 2.1$ fm^{-1}, is nicely illustrated in Fig. 4, which shows the RG evolution as the cutoff is successively lowered in the ^{3}S$_1$ partial wave.

Next, we analyze the scaling properties of $V_{\mathrm{low\,k}}$. For this purpose, we show matrix element $V_{\mathrm{low\,k}}(0,0)$ versus cutoff in Fig. 5 for the ^{1}S$_0$ and ^{3}S$_1$ partial waves. The main results are the following. T matrix preservation guarantees that $V_{\mathrm{low\,k}}(0,0)$ flows toward the scattering length as the cutoff is taken to zero, these are $a_{^1\mathrm{S}_0} = -23.73$ fm and $a_{^3\mathrm{S}_1} = 5.42$ fm and are well reproduced with $V_{\mathrm{low\,k}}$.

For cutoffs $\Lambda > m_\pi$, $V_{\mathrm{low\,k}}$ is nearly independent of the cutoff in the ^{1}S$_0$ channel and weakly linearly dependent in the ^{3}S$_1$ channel. According to EFT principles, the couplings are nearly independent of the cutoff as long as Λ is large enough to explicitly include the relevant degrees of freedom needed to describe the scale one is probing. Thus, the running of $V_{\mathrm{low\,k}}$ initiated at $\Lambda \sim m_\pi$ is a result of integrating out the pion. The rapid changes at very small Λ are the result of the large scattering length. To illustrate the effects of the large scattering length, we solve the RG equation for $V_{\mathrm{low\,k}}(0,0)$ for small cutoffs, with the ^{1}S$_0$ scattering length as the $\Lambda = 0$ boundary condition. One finds

$$V_{\mathrm{low\,k}}(0,0) \approx \frac{1}{1/a_{^1\mathrm{S}_0} - 2\Lambda/\pi}, \tag{9}$$

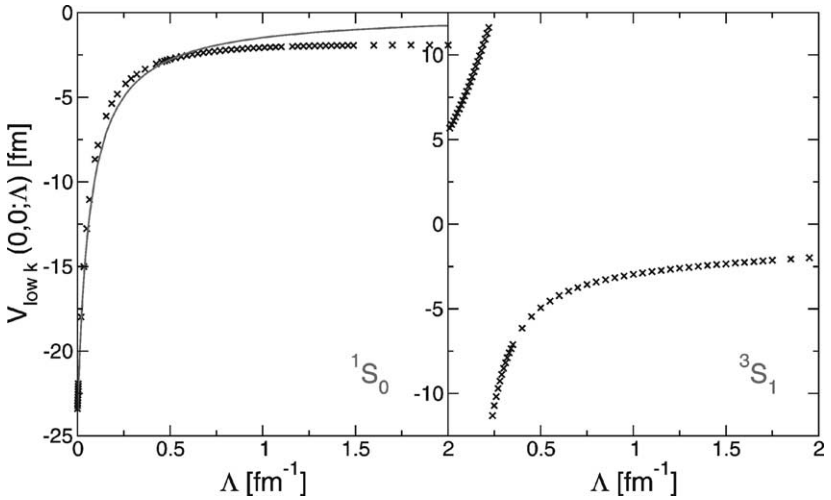

Fig. 5. RG flow of $V_{\mathrm{low\,k}}(0,0;\Lambda)$ versus cutoff Λ in the $^1\mathrm{S}_0$ and $^3\mathrm{S}_1$ partial waves. The solid line represents the solution of the RG equation for small Λ as discussed in the text.

which is shown as the solid curve in Fig. 5. Clearly, the agreement for small $\Lambda < m_\pi/2$ is convincing. Eq. (9) is identical to the Kaplan–Savage–Wise solution for the renormalization of the momentum-independent contact term in the pionless EFT, upon identifying Λ with the regulator mass μ used in dimensional regularization [8]. The weak dependence on the cutoff in the $^3\mathrm{S}_1$ partial wave results from the dominantly second order tensor contributions, which are peaked at relative momenta $k \approx 2$ fm^{-1} [26].

Finally, we note that $V_{\mathrm{low\,k}}$ preserves all scattering and bound states with energy $|E| < \Lambda^2$. Therefore, the jump in the $^3\mathrm{S}_1$ channel is the bound state contribution to the T matrix and occurs at $\Lambda = k_\mathrm{D} = \sqrt{m E_\mathrm{D}/\hbar^2} = 0.23$ fm^{-1}. From effective range theory and the Low equation [27], we have for the bound state contribution and thus the discontinuity

$$\Delta V_{\mathrm{low\,k}}(0,0;k_\mathrm{D})_{^3\mathrm{S}_1} = \frac{4}{\pi\, k_\mathrm{D}(1-k_\mathrm{D} r_0)} = 22.8 \text{ fm}, \tag{10}$$

where $r_0 = 1.75$ fm denotes the effective range in $^3\mathrm{S}_1$. This is in very good agreement with our results.

4. Summary

In this Letter, we have shown that the separation of scales in the nuclear force can be successfully applied to derive a model-independent low momentum nucleon–nucleon interaction. $V_{\mathrm{low\,k}}$ is obtained by integrating out the high momentum components of various potential models, leading to a physically equivalent effective theory in the low momentum Hilbert space. The decimation filters the details of the assumed short-distance dynamics of the bare interactions, provided one requires that the low energy observables are preserved under the RG. We have argued and provided numerical evidence that the model-independence of $V_{\mathrm{low\,k}}$ is a consequence of the common long-range OPE interaction and the reproduction of the same elastic scattering phase shifts. The momentum scale $\Lambda \sim 2.1$ fm^{-1}, corresponding to laboratory energies $E_\mathrm{lab} \sim 350$ MeV, is precisely the scale at which the low momentum interaction becomes independent of the input models. Our Letter demonstrates that the differences in the high momentum components of the nucleon force are not constrained by fits to the low energy phase shifts and the deuteron properties.

$V_{\mathrm{low\,k}}$ does not have high momentum modes, which are related to the strong, short range-repulsion in conventional models. Therefore, the low momentum interaction is considerably softer than the bare interactions (both in a plane-wave and an oscillator basis) and does not have a repulsive core. As a consequence, when $V_{\mathrm{low\,k}}$ is used as the microscopic input in the many-body problem, the high momentum effects in the particle–particle channel do not have to be ad-

dressed by performing a Brueckner ladder resummation or short-range correlation methods. In fact, with a cutoff on relative momenta, the phase space in the particle–particle channel is comparable to the particle–hole channels, and it would seem strange to resum the particle–particle channel, while the particle–hole channels are treated perturbatively in a hole–line expansion.

The use of $V_{\mathrm{low\,k}}$ in microscopic nuclear many-body calculations leads to model-independent results. $V_{\mathrm{low\,k}}$ has been successfully used as shell model effective interaction in model space calculations for two valence particle nuclei such as ^{18}O and ^{134}Te [28]. The starting point of these calculations has traditionally been the Brueckner G matrix, which depends on the bare V_{NN} used as well as the particular nuclei via the Pauli blocking operator. By means of $V_{\mathrm{low\,k}}$, the same low momentum interaction is used in different mass regions. $V_{\mathrm{low\,k}}$ has further been incorporated into Fermi liquid theory. This connects the low momentum interaction in free space and the quasiparticle interaction in normal Fermi systems. Two constraints have been derived which relate the Fermi liquid parameters of nuclear matter to the S-wave low momentum interaction at zero relative momentum [29]. Finally, adopting the RG approach to Fermi systems proposed by Shankar, $V_{\mathrm{low\,k}}$ is taken as the input to microscopic calculations of the quasiparticle interactions and the pairing gaps in neutron matter [30]. From the success of these applications, we believe that the model-independent $V_{\mathrm{low\,k}}$ is a very promising starting point for microscopic nuclear many-body calculations.

Few-body calculations with $V_{\mathrm{low\,k}}$ are in progress. Preliminary results for the ground state energies of triton and ^{3}He show that the three-body force for $V_{\mathrm{low\,k}}$ is weaker than, e.g., the conventional three-body force constructed for the Argonne potential.

Acknowledgements

We thank Gerry Brown for his encouragement and many stimulating discussions. This work was supported by the US DOE grant DE-FG02-88ER40388, the US NSF grant PHY-0099444 and by the Ramon Areces Foundation of Spain.

References

[1] M. Lacombe, et al., Phys. Rev. C 21 (1980) 861.
[2] R. Machleidt, K. Holinde, C. Elster, Phys. Rep. 149 (1987) 1.
[3] V.G.J. Stoks, et al., Phys. Rev. C 49 (1994) 2950.
[4] R.B. Wiringa, V.G.J. Stoks, R. Schiavilla, Phys. Rev. C 51 (1995) 38.
[5] R. Machleidt, F. Sammarruca, Y. Song, Phys. Rev. C 53 (1996) 1483.
[6] R. Machleidt, Phys. Rev. C 63 (2001) 024001.
[7] C. Ordonez, L. Ray, U. van Kolck, Phys. Rev. Lett. 72 (1994) 1982.
[8] D.B. Kaplan, M.J. Savage, M.B. Wise, Nucl. Phys. B 534 (1998) 329.
[9] T.-S. Park, et al., Phys. Rev. C 58 (1998) 637.
[10] E. Epelbaum, W. Glockle, U.-G. Meissner, Nucl. Phys. A 671 (2000) 295.
[11] S.R. Beane, et al., in: M. Shifman (Ed.), At the Frontier of Particle Physics, Vol. 1, World Scientific, p. 133, nucl-th/0008064.
[12] D.R. Entem, R. Machleidt, Phys. Lett. B 524 (2001) 93.
[13] G.P. Lepage, How to Renormalize the Schrödinger Equation, Lectures given at 9th Jorge Andre Swieca Summer School: Particles and Fields, São Paulo, Brazil, February 1997, nucl-th/9706029.
[14] T.T.S. Kuo, S.Y. Lee, K.F. Ratcliff, Nucl. Phys. A 176 (1971) 65.
[15] T.T.S. Kuo, E. Osnes, Folded-Diagram Theory of the Effective Interaction in Nuclei, Atoms and Molecules, in: Lecture Notes in Physics, Vol. 364, Springer, Berlin, 1990, p. 1.
[16] S.K. Bogner, A. Schwenk, T.T.S. Kuo, G.E. Brown, nucl-th/0111042.
[17] S.Y. Lee, K. Suzuki, Phys. Lett. B 91 (1980) 173.
[18] K. Suzuki, S.Y. Lee, Prog. Theor. Phys. 64 (1980) 2091.
[19] S.K. Bogner, T.T.S. Kuo, L. Coraggio, Nucl. Phys. A 684 (2001) 432c.
[20] M.C. Birse, J.A. McGovern, K.G. Richardson, Phys. Lett. B 464 (1999) 169.
[21] S.K. Bogner, T.T.S. Kuo, Phys. Lett. B 500 (2001) 279.
[22] V.G.J. Stoks, et al., Phys. Rev. C 48 (1993) 792.
[23] S.K. Bogner, T.T.S. Kuo, A. Schwenk, Phys. Rep. 386 (2003) 1.
[24] E. Epelbaum, et al., Nucl. Phys. A 645 (1999) 413.
[25] T. Neff, Ph.D. Thesis, Darmstadt University, 2002.
[26] G.E. Brown, Unified Theory of Nuclear Models and Forces, 3rd Edition, North-Holland, Amsterdam, 1971.
[27] G.E. Brown, A.D. Jackson, The Nucleon–Nucleon Interaction, North-Holland, Amsterdam, 1976.
[28] S.K. Bogner, et al., Phys. Rev. C 65 (2001) 051301(R).
[29] A. Schwenk, G.E. Brown, B. Friman, Nucl. Phys. A 703 (2002) 745.
[30] A. Schwenk, B. Friman, G.E. Brown, Nucl. Phys. A 713 (2003) 191.